4-1-2001

Geocoronal H-A [Alpha] Intensity Measurements Using the Wisconsin H-A [Alpha] Mapper Fabry-Perot Facility

S. Nossal
University of Wisconsin - Madison

F. L. Roesler
University of Wisconsin - Madison

J. Bishop
Naval Research Laboratory

R. J. Reynolds
University of Wisconsin - Madison

M. Haffner
University of Wisconsin - Madison

See next page for additional authors

JOURNAL OF GEOPHYSICAL RESEARCH, VOL. 106, NO. A4, PAGES 5605–5616, APRIL 1, 2001

Geocoronal Hα intensity measurements using the Wisconsin Hα Mapper Fabry-Perot facility

S. Nossal,[1] F. L. Roesler,[1] J. Bishop,[2] R. J. Reynolds,[3] M. Haffner,[3] S. Tufte,[3] J. Percival,[4] and E. J. Mierkiewicz[5]

Abstract. The Wisconsin Hα Mapper (WHAM), a remotely operable, semi-automated Fabry-Perot located at Kitt Peak Observatory, has been making an all-sky survey of interstellar hydrogen Balmer α (Hα) emissions since 1997. Using the annular summing spectroscopy technique, WHAM has acquired ~37,000 spectra to date, spanning almost 100 nights of observations. Since all of the galactic emission spectral data contain the terrestrial Hα (6562.7 Å) emission line, these measurements constitute a rich source of geocoronal data for investigating natural variability in the upper atmosphere. The WHAM observations also serve as a benchmark for comparison with future data. Analysis of the first year of WHAM data shows only small day-to-day variations after shadow altitude variations are taken into account. For example, at shadow altitudes of 2000 and 3000 km, the RMS scatter is within approximately +/− 20%; this variability is expected to be reduced with accurate accounting of the smaller-scale effects of observational slant path, zenith angle, and azimuth on the Hα intensity. This result is consistent with past midlatitude Wisconsin data sets but different from observations made by other observers and instruments at the low-latitude Arecibo site. The multiple viewing geometries of the observations provide stringent modeling constraints, useful in testing current modeling capabilities. Modeling of the WHAM data with a global nonisothermal resonance radiation transport code (*lyao_rt*) indicates that the signal-to-noise of the data is sufficient to determine relative variations in upper atmospheric atomic hydrogen column densities to better than 5%. This paper describes the WHAM aeronomy program and its observational scheme, analysis procedures, and results from data taken in 1997. Case study comparisons are made with past data sets and with predictions from the *lyao_rt* resonant radiation transport modeling code of *Bishop* [1999].

1. Introduction

The exosphere, the uppermost layer of the Earth's atmosphere, is a region uniquely characterized by low constituent densities and non-Maxwellian kinetic distributions in which atoms follow orbital trajectories between particle collisions [see, e.g., *Chamberlain and Hunten*, 1987]. Atomic hydrogen is distributed throughout the exosphere and becomes increasingly dominant with altitude. The main geocoronal Balmer α (Hα) emission process is fluorescence following solar Lyman β (resonance) excitation. Thus the changing height of the Earth's shadow provides a means to probe the vertical structure of the exosphere. The high-altitude (~450 km and above) and low-emission intensities at visible wavelengths (~1–20 R for geocoronal Hα) make the exosphere a difficult region to observe from the ground. Nevertheless, the Hα emission line (6562.7 Å) has been one of the primary observational signatures for geocoronal studies, particularly when measured using Fabry-Perot spectrometers [*Atreya et al.*, 1975; *Meriwether et al.*, 1980; *Yelle and Roesler*, 1985; *Shih et al.*, 1985; *Kerr et al.*, 1986, 2001a, 2001b; *Harlander and Roesler*, 1989; *He et al.*, 1993; *Nossal et al.*, 1993, 1997, 1998; *Bishop et al.*, 2001]. Geocoronal Hα measurements offer a means for assessing upper atmospheric variability, including its response to changes in solar and geophysical conditions.

Ongoing measurements of Hα intensities spanning more than a solar cycle have been independently compiled and analyzed from the Arecibo Observatory [*Kerr et al.*, 2001a, 2001b] and from Wisconsin [*Nossal et al.*, 1993], with the data from Arecibo showing considerably more variability. *Kerr et al.* [2001a] report that their observations from Arecibo display geocoronal Hα emission magnitudes varying by factors of ~2 within a period of a few days and that intensities are typically 50% greater under solar minimum than under solar maximum conditions for solar depression angles between 15° and 35° [*Kerr et al.*, 2001a]. Furthermore, *Kerr et al.* [2001b] have reported an approximate doubling of the geocoronal Hα emission for periods immediately following the onset of moderate geomagnetic storm conditions and an overall upward trend in the Arecibo long-timeline geocoronal Hα data set. In contrast, the observations from Wisconsin taken over a solar cycle show only a weak suggestion of solar activity dependence in Hα intensities. The data were not inconsistent with an overall upward climatic trend; however, any such trend has not yet been shown to be statistically significant [*Nossal et al.*, 1993]. As a wider range of solar geophysical conditions are sampled

[1]Physics Department, University of Wisconsin-Madison.
[2]E. O. Hulburt Center for Space Research, Naval Research Laboratory, Washington, D. C.
[3]Astronomy Department, University of Wisconsin-Madison.
[4]Space Astronomy Laboratory, University of Wisconsin-Madison.
[5]Department of Atmospheric and Oceanic Sciences, University of Wisconsin-Madison.

Paper number 2000JA000003.
0148-0227/01/2000JA000003$09.00

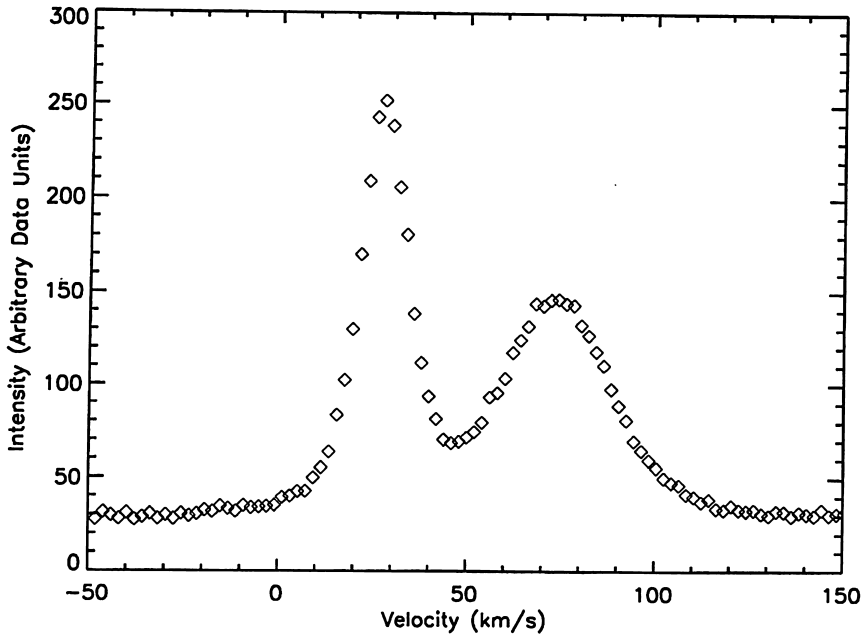

Figure 1. Sample Wisconsin Hα Mapper (WHAM) Hα nightsky spectrum, showing the geocoronal emission line (tall, narrow peak) superimposed on the galactic emission. Spectral displacement (horizontal axis) is expressed in velocity units. Zero velocity is placed at an arbitrary location. Intensity (vertical axis) is expressed in arbitrary intensity units. Emission line intensities are determined through comparisons with data from a nebular calibration source; the geocoronal Hα emission intensity in this spectrum is 5.5 R. Geocoronal line widths are not resolved in the WHAM data. The integration time for this profile was 30 s.

with time, data from the Wisconsin Hα Mapper (WHAM) Fabry-Perot should help to confirm or refute the hints of trends noted above in the midlatitude Wisconsin observations. The explanation is still outstanding for the difference in the degree of variability seen in the intensities observed from Arecibo and Wisconsin.

The WHAM Fabry-Perot, located at Kitt Peak, Arizona, has been acquiring an extensive body of geocoronal Hα emission data since 1997. Approximately 37,000 Hα spectra in multiple viewing geometries have been recorded to date, with significantly improved signal-to-noise and consistent relative and absolute calibration. Most of these data are the terrestrial Hα emission line components of galactic survey observations taken in the course of making an all-sky map of interstellar Hα emissions (Figure 1). A number of observations programmed specifically for exospheric studies have also been performed. WHAM Hα observations are continuing, though at a reduced rate due to WHAM science objectives involving other emission lines. The Wisconsin Hα Mapper data collected to date augment past Hα data sets by providing unprecedented daily and look direction coverage. Over 60 nights of observations were collected by WHAM during 1997, providing more comprehensive daily coverage than previous data sets and forming a baseline for future WHAM observations. Solar geophysical conditions were relatively quiet during this year as the solar cycle was coming out of its minimum phase; WHAM Hα measurements are scheduled to continue through at least the year 2002 and thus span the solar cycle through the current maximum. The WHAM Hα data offer a unique opportunity for systematic investigation of natural variability in the upper atmosphere.

The multiple viewing geometries used in taking the WHAM data provide stringent constraints for exospheric emission modeling. Given the high signal-to-noise and multiple viewing geometries of the WHAM data, coupled with improved capabilities for analysis of ground-based Hα data [*Bishop et al.*, 2001], reliable determination of upper atmospheric hydrogen abundances is feasible.

This paper describes the WHAM aeronomy program and its observational scheme, analysis procedures, and results from data taken in 1997. Case study comparisons are made with past data sets and with predictions from the *lyao_rt* resonant radiation transport modeling code of *Bishop* [1999].

2. Observations

2.1. Instrument Description

The Wisconsin Hα Mapper is a remotely operable, large aperture (15 cm), double-etalon Fabry-Perot spectrometer coupled to a charge-coupled device (CCD) camera [*Tufte*, 1997; *Reynolds et al.*, 1998]. The Fabry-Perot is particularly well suited for high-resolution studies of faint, diffuse sources such as the geocorona as it simultaneously achieves high resolution and high throughput. The second etalon provides superior off-band rejection by extending the free spectral range of the instrument, minimizing Fabry-Perot ghosts and increasing the instrumental contrast by suppressing multiple orders in the interference pattern [*Roesler*, 1974]. WHAM operates at a resolving power of 25,000, with a resulting resolution of 12 km s^{-1} (0.26 Å at Hα), which is sufficient for separation of the Doppler-shifted galactic line and the geocoronal line components and retrieval of the airglow intensities.

The Wisconsin Hα Mapper Fabry-Perot is similar in design to the double-etalon Fabry-Perot instruments used for past Wisconsin Hα intensity observations. However, previous instruments used photomultiplier detection rather than the CCD

imaging-based annular summing detection used for WHAM; for the resolution of the WHAM instrument, the latter advance has yielded a roughly fiftyfold increase in sensitivity, leading to integration periods of only ~30 s per Hα spectrum. Two factors contribute to the gains achieved with the annular summing technique: Many elements are recorded at once (i.e., multichannel detection), and the quantum efficiency of the low noise, cryogenically cooled CCD at Hα (~78%) is about a factor of 4 greater than that for photomultipliers [*Coakley et al.*, 1996; *Nossal et al.*, 1997; *Reynolds et al.*, 1990]. Owing to the multichannel detection, variations in airglow intensities occurring during an integration affect all spectral channels equally.

The etalons used in WHAM have broadband coatings with a reflectivity of ~91%. Using a pressure control system and sulfur hexafluoride gas, the spectral window can be set to any 200 km s^{-1} range (4.375 Å at Hα) between 4800 and 7200 Å. The Fabry-Perot is coupled to a siderostat (a 0.6-m "light bucket" telescope), which provides a 1° diameter beam on the sky. WHAM is remotely operable from Wisconsin using the messaging system developed for the 3.5-m Wisconsin-Indiana-Yale-NOAO (WIYN) telescope at Kitt Peak, Arizona [*Percival*, 1995].

2.2. The WHAM Observing Scheme

WHAM's primary scientific mission is to make an all-sky survey of Hα emission intensities from the interstellar medium [*Reynolds*, 1997, 1984]. As such, most of the WHAM Hα observations are made in a sequence rastering over a particular block on the sky. Usually, observations are made over several adjacent blocks before moving to another part of the sky. However, sometimes a stray block is observed separately in order to make up for a hole left during a previous sequence of observations. In addition, a region of low galactic emission (the ~.2 R Lockman region at right ascension (RA) 10.91; declination (DEC) 57.92) is monitored on most observation nights. We use the terrestrial Hα emission present in all of these interstellar Hα spectra.

A small portion of the WHAM observations are made in observing directions specifically designed for geocoronal studies, with the majority of these being zenith data. WHAM makes only a few zenith observations per night, fit around the astronomical observing schedule. We then consolidate these zenith spectra and plot them by month. During special campaigns, WHAM has taken extra observations specifically designed for exospheric investigations.

2.3. Calibration

Absolute intensity calibration of the Wisconsin Hα Mapper observations is made through comparison with astronomical nebular emission sources, all of which have been tied to the North American Nebula (NAN). This method has been used for calibrating all of the Wisconsin-based aeronomical, planetary, and astronomical hydrogen Hα observations, and thus this method provides for internal consistency between the data sets. Nebular calibration offers the advantage of long-term source stability and calibration by line rather than continuum emission [*Nossal et al.*, 1993]. Nebular sources are also diffuse and fill the Fabry-Perot's field of view in much the same manner as the geocorona. In addition, as these sources are outside of the Earth's atmosphere, they are subject to the same atmospheric extinction as the geocorona, minimizing this source of uncertainty. NAN has been calibrated for Hα using standard stars [*Scherb*, 1981] and has also been checked against a blackbody source [*Nossal*, 1994]. The Hα emission intensity of the (0.8°) patch of NAN viewed by the Wisconsin scanning Fabry-Perot instruments was measured to be 850 +/− 50 R.

Currently associated with the WHAM observations, there is about a 5% uncertainty in the calibration of the relative Hα intensity and a conservative 20% uncertainty in the absolute value of this intensity. The larger uncertainty in the WHAM absolute Hα calibration is due to its larger field of view (1°) as compared with that of the Wisconsin scanning instruments (0.8°). Our estimate of the intensity corresponding to the 1.0° patch of NAN is 800 +/− 160 R. However, this uncertainty should be reduced following planned recalibration experiments.

The spectral dispersion across the CCD chip was calibrated using images from a Dα-Hα laboratory hollow cathode lamp source [*Tufte*, 1997]. The spectral increment per data point was then calculated using the spectral separation between the two emissions.

A thorium 6554 Å line was used to obtain a measure of the instrumental profile by observing its emission at a ring radius close to that used for making the night sky Hα observations [*Tufte*, 1997; *Coakley et al.*, 1996; *Nossal et al.*, 1997]. The thorium 6554 Å line was chosen because it is the brightest thorium emission in the spectral vicinity of Hα and because it is a narrow line whose width is approximately 1/40 that of the geocoronal Hα emission.

3. Data Analysis

Figure 1 shows an example Hα line spectrum from the WHAM Hα survey, displayed in arbitrary intensity units versus spectral displacement. The integration time for this profile was 30 s, and the geocoronal Hα emission line intensity was 5.5 R. The tall, narrow peak results from the geocorona, and the broader, shorter peak is the galactic emission. Spectral displacements are expressed here in velocity units (an interval of 1 km s^{-1} corresponds to 0.0219 Å or 0.0508 cm^{-1} at Hα), which is useful for indicating Doppler shifts between the galactic and geocoronal emissions. The "zero" velocity point on Figure 1 is arbitrary. Hα emission intensities are determined by comparing the integrated area of a night sky emission line with that from the nebular calibration source. At this instrumental resolving power, the geocoronal Hα line width is not resolved; high-resolution experiments have shown the width to be ~6–8 km s^{-1} [see, e.g., *Nossal et al.*, 1997].

In processing each measurement, dark counts, the bias, and cosmic ray hits are first removed from the CCD image of the Fabry-Perot interference pattern. The CCD image is then adjusted for pixel-to-pixel sensitivity variations and for vignetting within the instrument using a white light flat field. Using the property that equal-area annuli in the Fabry-Perot fringe pattern correspond to equal spectral intervals, the image is converted to a line profile (please see Figure 1) by summing the intensities of the pixels lying in equal area annular bins. The size of the annular bin is selected so as to sample several times within each resolution element. More details about these procedures are given by *Coakley et al.* [1996] and *Nossal et al.* [1997].

3.1. Intensity Retrievals

To process the large quantity of WHAM survey data, fits were made using single Gaussians to approximate the geocoronal emission line shape. One profile per block of survey ob-

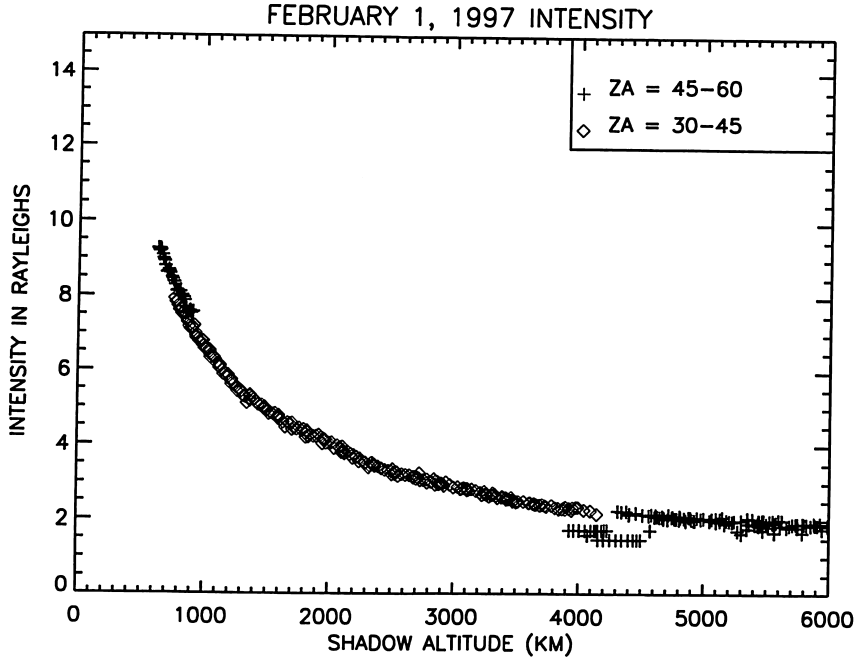

Figure 2. Representative WHAM geocoronal Hα intensities versus shadow altitude, from the night of February 1, 1997. The discontinuity at the low shadow altitudes is due to viewing geometry differences; that at ~4200 km is due to the overlap between the geocoronal and galactic emission lines. Please see text for further explanation.

servations was manually fit, and the others in the block were fit in a batch job format using starting inputs from the initial fit. The majority of survey observations are planned for times which minimize overlap (i.e., maximize the Doppler shift) between the geocoronal and galactic Hα emission components. When overlaps did arise, the geocoronal width was sometimes held fixed in order to achieve a more accurate overall fit to the galactic emission. In such cases the accuracy of the geocoronal intensity may be compromised (please see, for example, the discontinuity at 4200 km in Figure 2).

The zenith data, taken specifically for exospheric studies, are fit individually using two linked Gaussians of fixed spectral spacing and relative areas corresponding to the fine structure components directly excited in solar Lyman β scattering [see, e.g., *Nossal et al.*, 1998]. Overlaps between the geocoronal and galactic emission components in the zenith data are handled using an iterative fitting procedure.

While sufficient for geocoronal Balmer line intensity measurements, the spectral resolution of the WHAM instrument is too low for line profile studies. Thus it is not possible to resolve the cascade contribution from scattering of the higher lying solar Lyman lines [*Yelle and Roesler*, 1985; *Chamberlain*, 1987; *Meier*, 1995; *Nossal et al.*, 1998]. Cascade excitation rates have been calculated to contribute on the order of 4% of the low shadow altitude Hα emission at solar minimum (R. R. Meier, personal communication, 1999) using Solar and Heliospheric Observatory/Solar Ultraviolet Measurements of Emitted Radiation (SOHO/SUMER) solar Lyman line spectra [*Warren et al.*, 1998]. This estimate is lower than the 7% originally calculated by *Meier* [1995] from lower-resolution solar Lyman line spectra obtained from a 1962 sounding rocket flight [*Tousey*, 1963; *Tousey et al.*, 1964]. Previous high-resolution geocoronal Hα line profile measurements made under solar maximum conditions [*Nossal et al.*, 1998] indicated a cascade contribution of ~10%. The differences between the observed and predicted results remain unresolved. Observations in progress using higher-resolution Fabry-Perots at the Pine Bluff Observatory, Wisconsin, are expected to help determine the bounds of the cascade contribution with season and differing solar-geophysical conditions [*Mierkiewicz et al.*, 1999]. Such information can then be used to improve our fitting schemes for lower-resolution observations, such as the WHAM exospheric data.

Complications associated with atmospheric extinction and tropospheric scattering are minimized for WHAM by the clear air conditions at the high-altitude Kitt Peak Observatory site. Atmospheric extinction is largely accounted for since the exospheric source atoms and the nebular calibration source are both outside of the Earth's atmosphere. Uncertainties associated with atmospheric extinction are less than ~5% for observations included in this paper which were taken at zenith angles of less than 45° and less than ~7% for observations taken at zenith angles between 45° and 60°. Tropospheric scattering adjustments have been estimated using a radiative transfer model developed by *Leen* [1979] [see also *Shih et al.*, 1985]. This model uses a single scattering approximation and takes into account Rayleigh scattering by molecules, Mie scattering by aerosols, and the relatively small extinction from ozone absorption. The Leen correction method has been applied to the WHAM case study (Figure 2) and zenith (Figure 7) data but not yet to the bulk survey data (Figures 3 and 4). Tropospheric scattering corrections applied to the Hα intensities of Figure 2 ranged from ~13 to 18%, depending upon the observational look direction. Future data analysis will incorporate anticipated refinements to this scattering correction method.

3.2. Observed Intensity Variations

Since geocoronal Hα is primarily excited by solar Lyman β radiation, the dominant variation seen at a ground facility

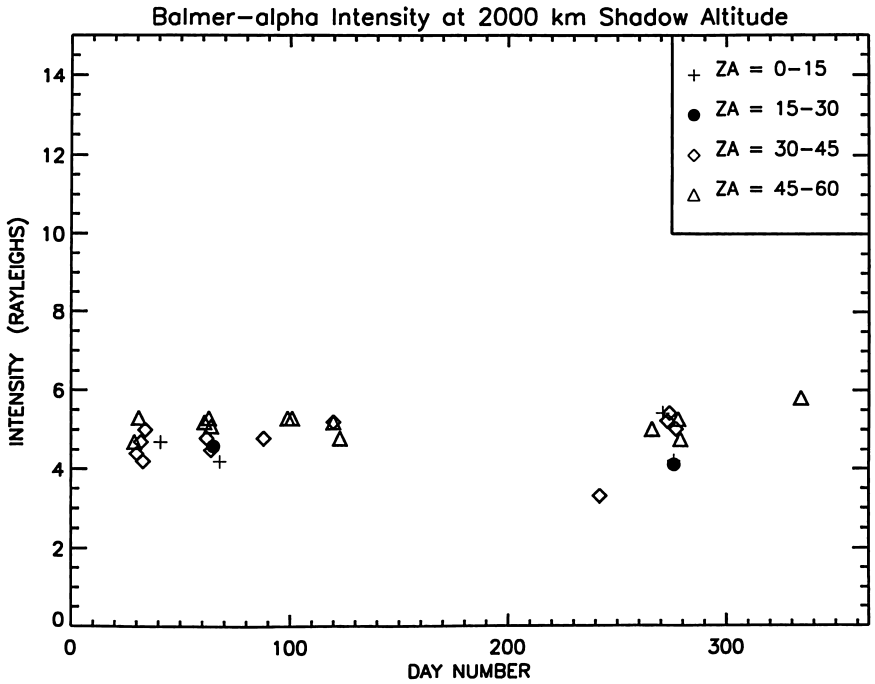

Figure 3. Upper atmospheric Hα intensities at 2000-km shadow altitude plotted versus day number for the year 1997. Viewing geometry variations likely account for most of the apparent scatter.

during a given night is typically that associated with line-of-sight shadow height variations. A representative WHAM geocoronal Hα intensity versus shadow altitude curve is shown in Figure 2. These data were taken on February 1, 1997, as part of the galactic Hα survey. The shadow altitude is determined by the optical depth of solar Lyman β radiation and the observational look direction. Solar Lyman β is fully absorbed by atmospheric O_2 below 102 km. Thus, for Lyman β excitation the Earth's shadow forms a cylinder with a radius that is 102 km greater than that of the Earth. The shadow altitude is the altitude of the location where the observational line of sight pierces this cylinder. Changes in intensity related to observational slant path zenith angle and azimuth variations for a constant shadow height can also be significant. The multidimensions of the viewing geometry coordinates make data display challenging.

To partially address these viewing geometry dependences, we have separated the data into four zenith angle bins: 0°–15°,

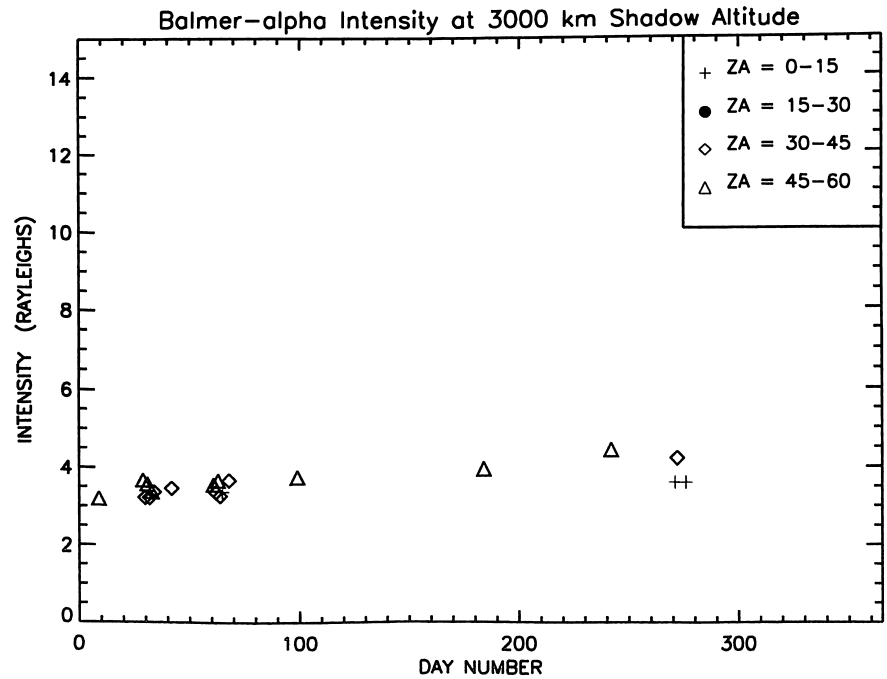

Figure 4. Same as Figure 3 but for 3000-km shadow altitude.

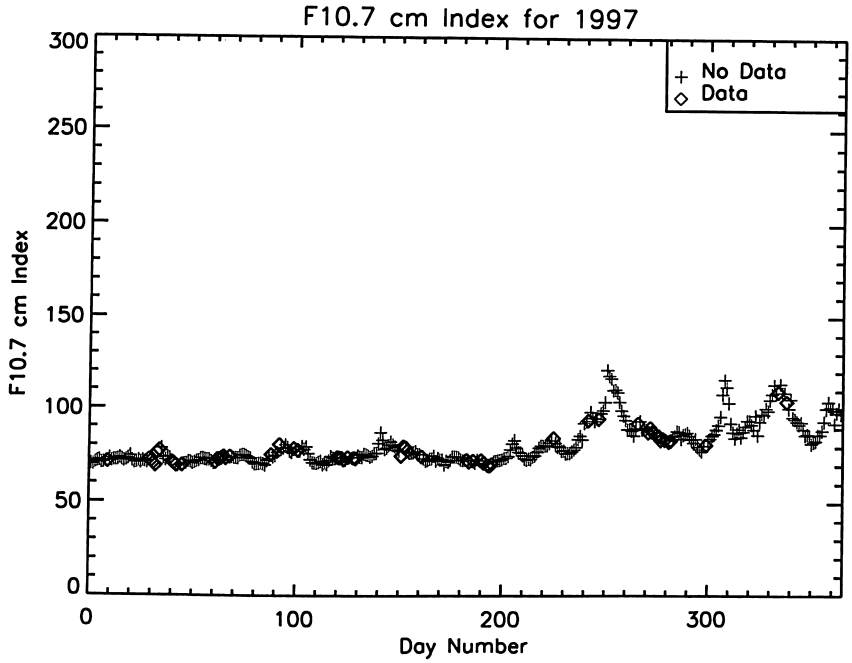

Figure 5. Daily solar $F10.7$ cm plotted versus day number for 1997. Values corresponding to WHAM observation dates are indicated with diamonds.

15°–30°, 30°–45°, and 45°–60°. The discontinuity seen at low shadow altitudes in Figure 2 is due to such viewing geometry differences. More pronounced intensity shifts (by as much as 2 R) can occur for small zenith angle shifts (3°–5°) at large zenith angles and low shadow altitudes. The discontinuity at ~4200 km in Figure 2 is due to overlap between the geocoronal and galactic emission lines. The overlap between these two emissions was too great to fit them each separately, and thus a fixed estimated area for the geocoronal emission was subtracted from the spectrum, leaving the galactic emission. This discontinuity provides feedback to the astronomical analysis, indicating that the adopted area value was underestimated for the geocoronal line and that the galactic data should be corrected.

In contrast, relatively little variation has been observed for shadow altitudes above ~1000 km, as seen in Figures 3 and 4 displaying the WHAM 1997 Hα survey intensities at shadow altitudes of 2000 and 3000 km, respectively, versus day number. (Here day 1 corresponds to January 1, 1997.) These intensity values at 2000 and 3000 km were read from plots of the survey data such as that displayed in Figure 2. Such determinations are within ~.25 R. Overall, the RMS scatter in Figures 3 and 4 is within about +/−20%; much of this scatter appears to be associated with observational viewing geometry dependencies and is anticipated to be reduced in future analysis refinements.

There is perhaps a hint of an upward trend in the WHAM intensities with increasing $F10.7$ value. However, in 1997 both solar and geophysical conditions were relatively quiet on most dates of data collection: $F10.7$ in 1997 increased gradually from ~70 to ~100 with minor fluctuations, and Ap on most dates was below 20. (Daily solar $F10.7$ and Ap geomagnetic index values for 1997 are plotted in Figures 5 and 6, with observation date values indicated by diamonds.) A few of our 1997 observations coincided with active (Ap = 16–29) or minor storm (Ap = 30–49) geomagnetic conditions, but none coincided with major geomagnetic storm conditions.

Comparison of zenith Hα observations taken with the Wisconsin Hα Mapper in January and February 1998 and zenith observations made from the Pine Bluff, Wisconsin Observatory, during the winter National Science Foundation–Collaborative H-alpha and Radar Measurements (NSF-CHARM) campaigns of the early 1990s (Figure 7) also show agreement to within ~10% in the value of their intensities, with the exception of a few high shadow altitude, low intensity data points. This agreement is within calibration uncertainties and is perhaps surprising given the large difference in solar activity levels between the two sets of measurements, with the WHAM data taken during solar minimum and the NSF-CHARM data acquired under solar maximum conditions with average $F10.7$ values of ~200. Though at different longitudes, both sets of observations are from midlatitude sites. This consistency and relative lack of solar activity–related variations have been noted in past comparisons of Wisconsin geocoronal Hα intensity measurements [*Nossal et al.*, 1993].

3.3. Atomic Hydrogen Abundance Retrievals

A case study of determining upper atmospheric nightside atomic hydrogen abundances using WHAM data was carried out with the February 1, 1997, data shown in Figure 2 and the *lyao_rt* code of *Bishop* [1999]. The *lyao_rt* code accounts for nonisothermal conditions and multiple as well as single scattering excitation by solar Lyman emissions, but this code does not account for the complications of cascade, collisional excitations, or exospheric kinetics. Thermospheric density and temperature profiles are obtained from the Mass Spectrometer Incoherent Scatter–90 (MSIS-90) upper atmospheric empirical model [*Hedin*, 1991]. MSIS atomic hydrogen density profile ($[H](z)$) predictions are not used in the radiative transport modeling, however. The atomic hydrogen density profile $[H](z)$ at thermospheric altitudes is now handled by direct integration of the vertical diffusion equation, as has been done in several past studies [e.g., *Anderson et al.*, 1987; *He et al.*, 1993], which typically results in thermospheric column abun-

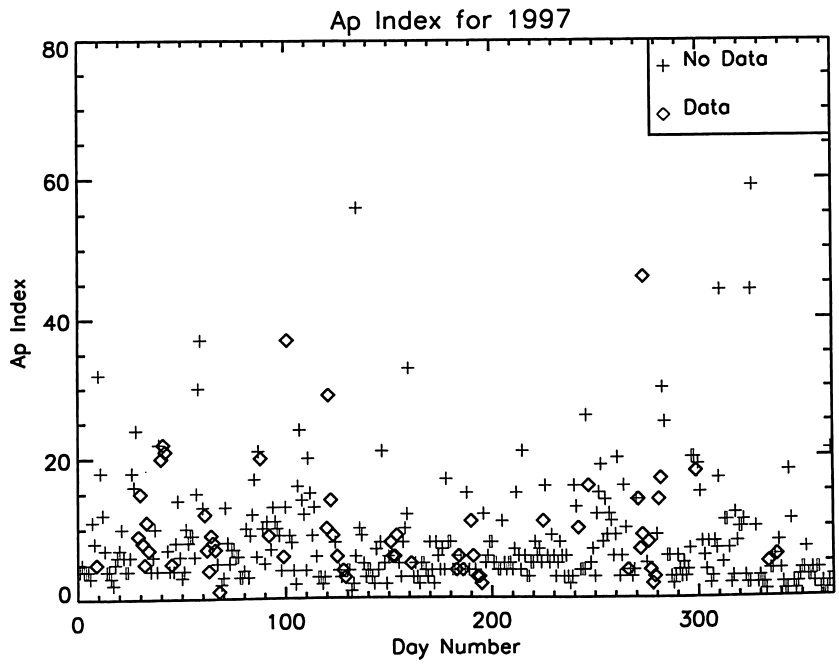

Figure 6. Daily *Ap* geomagnetic index plotted versus day number for 1997. Values corresponding to WHAM observation dates are indicated with diamonds.

dances larger than those generated by MSIS (sometimes by as much as factors of ~2).

Past modeling analyses of ground-based Hα data, typically acquired in the zenith or in observing schemes focusing on zenith angles confined to the Sun-Earth-zenith plane [*Shih et al.*, 1985; *Anderson et al.*, 1987], have struggled with obtaining atomic hydrogen density profiles using the exobase density as the main fit parameter in conjunction with assumed density profile shapes. With hindsight, most of these data sets do not provide sufficient modeling constraints to yield an unambiguous profile determination, so that data analysis focused on apparent discrepancies in derived exobase density values. A partial exception is presented by the data collected in multiple viewing geometries at the clear air Haleakala, Hawaii, observing site in February and October 1988 [*Harlander and Roesler*, 1989]. Modeling of these data with the *lyao_rt* code and updated solar Lyman line fluxes [*Warren et al.*, 1998; *Woods and Rottman*, 1997] yielded firmer estimates of upper thermo-

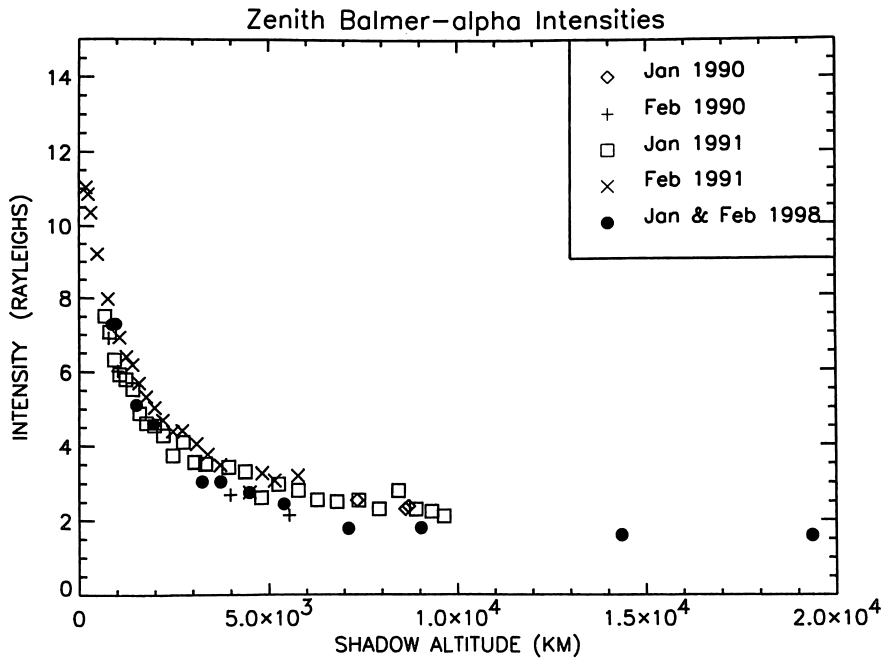

Figure 7. WHAM solar minimum January–February 1998 zenith data (solid circles) compared to solar maximum zenith data taken during January and February of 1990 and 1991 at the Pine Bluff, Wisconsin Observatory.

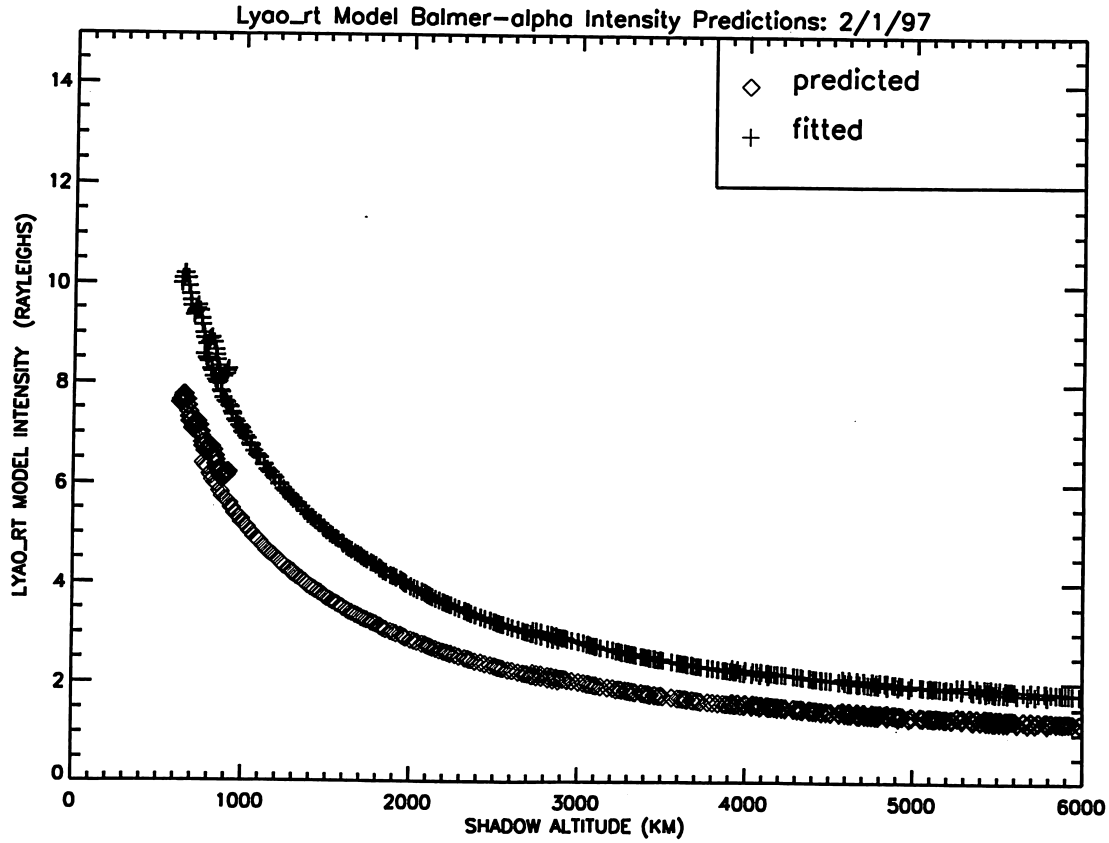

Figure 8. Model intensities versus shadow altitude for the WHAM observations taken on February 1, 1997, comparing a *lyao_rt* "best fit" computed with a nightside-averaged atomic hydrogen density distribution having a thermospheric plus exospheric column abundance of 12.1×10^{13} cm^{-2} (upper curve) and model results for which the Mass Spectrometer Incoherent Scatter (MSIS) predicted exobase density (lower curve) has been used. The corresponding nominal exobase densities are 4.5×10^5 and 3.0×10^5 cm^{-3}, respectively.

spheric atomic hydrogen densities, so that in the case of the near-solar minimum February 1988 Haleakala measurements, estimates were completely consistent with AE-C satellite in situ determinations made under similar solar, geomagnetic, and location conditions [*Bishop et al.*, 2001]. The Haleakala Fabry-Perot was of similar design as WHAM but was run at a higher resolution and with photomultiplier rather than CCD detection.

However, even the Haleakala Hα data failed to provide sufficient constraints for the specification of [H](z) throughout the thermosphere. This is, in fact, a general limitation of ground-based Hα intensity data analyses: All observation slant paths pass through the entire emission region, making it far more difficult to obtain an unambiguous determination of [H](z) than is the case with limb-scanning measurements from a satellite-borne instrument. The high signal-to-noise, short integration times and the multiple shifts in look directions carried out in a typical measurement sequence bring the WHAM data much closer to providing the viewing geometry constraints needed for unambiguous [H](z) retrievals. Nevertheless, feasibility of comparison of the large number of WHAM Hα spectra, coupled with a desire to obtain an atomic hydrogen abundance measure more suitable for the study of atomic hydrogen abundance variations with respect to season, solar activity, and geomagnetic conditions, points to the use of thermospheric plus exospheric atomic hydrogen column densities as the main fit parameter. This choice is augmented by the fact that while optically thick, thermospheric Lyman β optical depths are not large, and the single scattering component of measured Hα typically remains an appreciable fraction of the total intensity for shadow altitudes out to beyond ~3000 km.

Figure 8 displays *lyao_rt* model intensities versus shadow altitude for the conditions of the February 1, 1997, WHAM observations ($F10.7 = 71.4$, $Ap = 5$), computed for each WHAM observation slant path and then grouped into the same zenith angle bins as those used in Figure 2. The line-center solar Lyman β excitation flux derived from SOHO/SUMER data as a solar minimum reference value, 5×10^9 photons cm^{-2} s^{-1} Å^{-1}, has been adopted without adjustment [*Warren et al.*, 1998]. Most of the WHAM measurements on this date were taken near local midnight. Radiative transport modeling in this case requires handling of transport variations throughout the nightside, which here has been approximated through the use of atomic hydrogen density profiles constructed by weighted composite of [H](z) profiles computed at numerous points around the terminator. Subsequent variation of the nightside-averaged [H](z) profile to obtain a "best fit" has been limited to adjustments in the exobase density value without explicit handling or adjustment of corresponding diffusive flux values. The signal-to-noise of the data is sufficient to determine relative variations in upper atmospheric atomic hydrogen column densities to better than 5%. Included in Figure 8 are *lyao_rt* Hα intensities versus shadow altitude for an

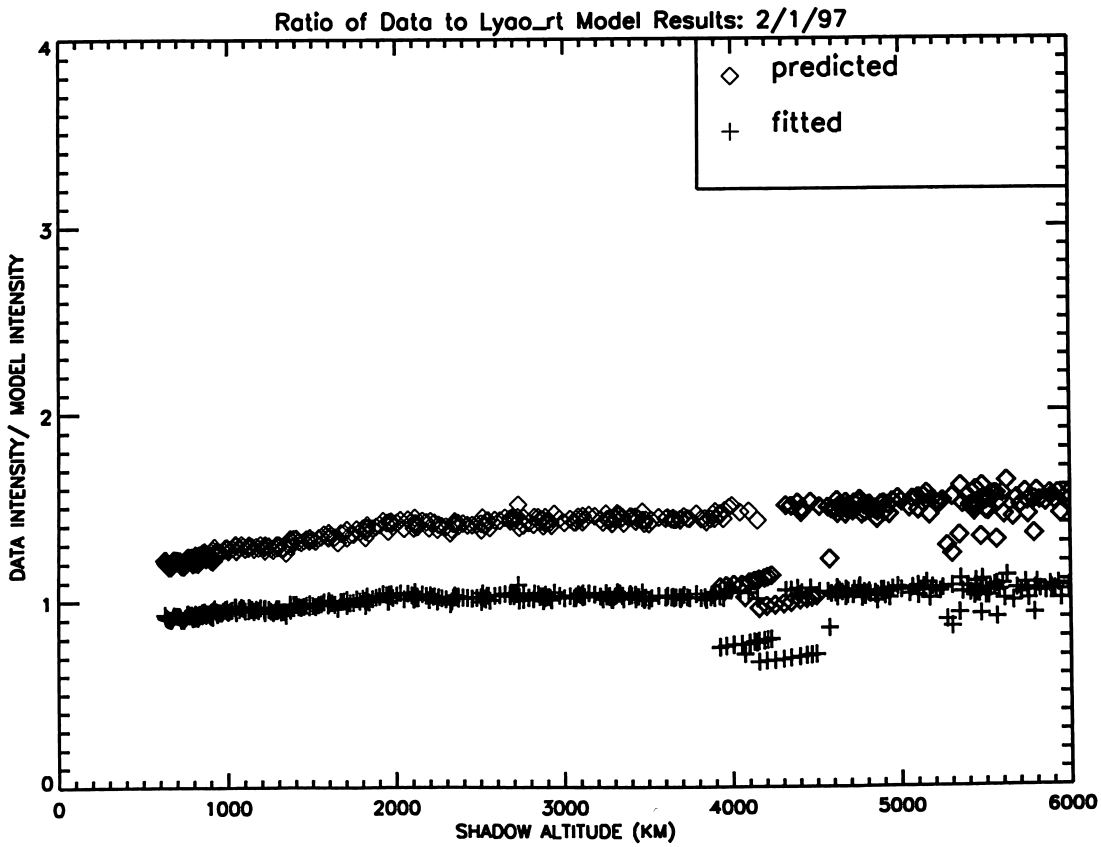

Figure 9. WHAM geocoronal Hα intensities from February 1, 1997 (Figure 2), ratioed to the corresponding *lyao_rt* model intensities of Figure 8.

[H](z) profile characterized by a nightside-averaged exobase density (3.0×10^5 cm^{-3}) predicted by MSIS for the WHAM observation conditions and corresponding "best fit" results obtained using a mean exobase density of 4.5×10^5 cm^{-3}; the corresponding thermospheric plus exospheric column abundances are 9.6×10^{13} and 12.1×10^{13} cm^{-2}, respectively, indicating an overall adjustment of ~20%, which is well within the combined uncertainties associated with WHAM calibration, the solar line-center Lyman β fluxes of *Warren et al.* [1998], and errors associated with the use of simplified nightside-averaged [H](z) profiles.

Data/model intensity ratios are shown in Figure 9. Aside from the discontinuity in the WHAM data at ~4200 km shadow altitude associated with terrestrial and galactic component overlap, the *lyao_rt* results for the approximate nightside-averaged "best fit" [H](z) profile show fairly uniform agreement over the entire shadow altitude range. The residual slant in the data/model curve may point to a need to adjust atomic hydrogen diffusive flux values as well as exobase density values in the fitting, but it will first be necessary to develop a more sophisticated handling of nightside Lyman β transport variations suitable for use in modeling the large volume of WHAM data. Nevertheless, the results shown in Figure 9 demonstrate that the signal-to-noise and use of multiple viewing geometries in the WHAM data present modeling constraints sufficiently strong to offer firmer determinations of nightside atomic hydrogen abundances than have been possible in the past.

4. Discussion

Data from the Wisconsin Hα Mapper Fabry-Perot address the issue of variability in upper atmospheric emissions at a new level of precision thanks to the high sensitivity, accurate calibration, frequent sampling, and improved modeling that is now available for examining the data. Analysis of the first year (1997) of WHAM geocoronal Hα emission data has yielded absolute intensities and only small daily intensity variations consistent with analyses of past Wisconsin data sets, once viewing geometry variations are taken into account. A RMS scatter in the geocoronal Hα intensity of within ~20% has been noted for comparisons of survey observations taken at the same look direction shadow altitude of 2000 or 3000 km; this is a conservative bound on the intrinsic variability since observational zenith angle and azimuthal viewing geometry effects still present in the data have been shown to produce scatter of this magnitude. Despite a large change in solar index, WHAM Hα intensities taken in the zenith direction during near solar minimum conditions agree to within ~10% (except for a few low-intensity points at high shadow altitudes) with the value of the intensities taken in the early 1990s during near solar maximum conditions, at midlatitude and also in the zenith direction. Case study comparisons with global resonance radiation transport modeling results indicate that the WHAM geocoronal data have sufficient signal-to-noise to distinguish and rank goodness of fit for different model scenarios to within 5% in their associated upper atmospheric hydrogen column abundance. The multiple viewing geometries of the WHAM data provide stringent modeling constraints. As a result, modeling of the total WHAM data set offers an opportunity to obtain firmer determinations of nightside atomic hydrogen abundances than has been possible in the analysis of past data sets. We anticipate that comparison of these retrieved column densities with those predicted from climate models will provide an

observational test of the upward hydrogen fluxes arising from modeled mesospheric and thermospheric hydrogenous species. An additional conclusion is that the geocoronal analysis can be fed back to improve analysis of galactic Hα measurements.

WHAM is scheduled to continue Hα observations through solar maximum to at least the year 2002, though at a reduced rate compared with its initial two years. The initial year of WHAM data coincided with solar minimum, relatively quiet conditions. The continuing WHAM Hα observations should provide solid measures of geocoronal Hα emission and the upper atmospheric hydrogen abundance variations associated with changes in solar activity.

Scientific goals of the WHAM aeronomy program include addressing the following questions: (1) What variabilities in upper atmospheric Hα emission are observed, and what are the associated variations in upper atmospheric atomic hydrogen abundances? (2) What effects relating to upper atmospheric hydrogen can be attributed to variations in solar-geophysical conditions? (3) How do upper atmospheric hydrogen abundances retrieved from the WHAM data compare with those obtained from the database underlying the empirical MSIS-90 model [*Hedin*, 1991] and with predictions from climatic models such as the TIMES GCM [*Roble and Ridley*, 1994]?

We anticipate that further knowledge of the natural variability in exospheric emissions will aid in efforts to isolate possible signs of change in the exosphere responding to human activity. Such potential signatures include a predicted~30–50% rise in exospheric hydrogen [*Ehhalt*, 1986; *Roble and Dickinson*, 1989; *CEDAR Steering Committee*, 1997] in response to a doubling of lower atmospheric methane concentrations, a primary greenhouse warming gas [*Houghton et al.*, 1995]. The high signal-to-noise of the data and the long-term stability of the nebular calibration sources attest to the value of the Wisconsin Hα Mapper Fabry-Perot observations as a benchmark reference data set.

Acknowledgments. The authors wish to thank J. Harlander and F. Scherb for their long-term and valuable contributions to the Wisconsin geocoronal research program. The work documented in this paper was supported by NSF grants AST9619424, ATM9415841, and ATM9813825.

Janet G. Luhmann thanks G. Randall Gladstone and other referees for their assistance in evaluating this paper.

References

Anderson, D. E., Jr., L. J. Paxton, R. P. McCoy, R. R. Meier, and S. Chakrabarti, Atomic hydrogen and solar Lymanα flux deduced from *STP* 78-1 UV observations, *J. Geophys. Res.*, *92*, 8759, 1987.

Atreya, S. K., P. B. Hayes, and A. F. Nagy, Doppler profile measurements of the geocoronal hydrogen Balmer alpha line, *J. Geophys. Res.*, *80*, 635, 1975.

Bishop, J., Transport of resonant atomic hydrogen emissions in the thermosphere and geocorona: Model description and applications, *J. Quant. Spectrosc. Radiat. Transfer*, *61*, 473, 1999.

Bishop, J., J. Harlander, S. Nossal, and F. L. Roesler, Analysis of Balmerα intensity measurements near solar minimum, *J. Atmos. Sol. Terr. Phys.*, in press, 2001.

CEDAR Steering Committee (Eds.), Coupling, energetics, and dynamics of atmospheric regions, *CEDAR Phase III Rep.*, Natl. Sci. Found., Upper Atmos. Res. Div., Arlington, Va., 1997.

Chamberlain, J. W., Balmer profiles in the geocorona and interstellar space, 1, Asymmetries due to fine structure, *Icarus*, *70*, 476, 1987.

Chamberlain, J. W., and D. M. Hunten, *Theory of Planetary Atmospheres: An Introduction to Their Physics and Chemistry*, 2nd ed., pp. 330–415, Academic, San Diego, Calif., 1987.

Coakley, M. M., F. L. Roesler, R. J. Reynolds, and S. Nossal, Fabry-Perot/CCD annular summing spectroscopy: Study and implementation for aeronomy applications, *Appl. Opt.*, *35*, 6479, 1996.

Ehhalt, D. H., On the consequence of a tropospheric CH_4 increase to the exospheric density, *J. Geophys. Res.*, *91*, 2843, 1986.

Harlander, J., and F. L. Roesler, Observations of geocoronal Balmer-alpha from Mt. Haleakala, Hawaii (abstract), *Eos Trans. AGU*, *70*, 1238, 1989.

He, X., R. B. Kerr, J. Bishop, and C. A. Tepley, Determining exospheric hydrogen density by reconciliation of H-alpha measurements with radiative transfer theory, *J. Geophys. Res.*, *98*, 21,611, 1993.

Hedin, A. E., Extension of the MSIS thermosphere model into the middle and lower atmosphere, *J. Geophys. Res.*, *96*, 1159, 1991.

Houghton, J. T., L. G. Meira Filbo, B. A. Callander, N. Harris, A. Kattenberg, and K. Maskell (Eds.), *Climate Change 1995: The Science of Climate Change*, Cambridge Univ. Press, New York, 1995.

Kerr, R. B., S. K. Atreya, J. W. Meriwether Jr., C. A. Tepley, and R. G. Burnside, Simultaneous hydrogen alpha line profile and radar measurements at Arecibo, *J. Geophys. Res.*, *91*, 4491, 1986.

Kerr, R. B., R. Garcia, X. He, R. Lancaster, J. Noto, R. A. Doe, C. A. Tepley, M. Lappen, B. McCormack, and J. Friedman, Periodic variations of geocoronal Balmer-alpha brightness due to solar driven exospheric abundance variations, *J. Geophys. Res.*, in press, 2001a.

Kerr, R. B., X. He, R. Lancaster, J. Noto, R. A. Doe, M. Lappen, B. McCormack, C. A. Tepley, R. Garcia, and J. Friedman, Secular variability of the geocoronal Balmer-alpha brightness: Magnetic activity and possible human influences, *J. Geophys. Res.*, in press, 2001b.

Leen, T., Application of radiative transfer theory to photometric studies of astronomical objects, M.S. thesis, Univ. of Wis., Madison, Wis., 1979.

Meier, R. R., Solar Lyman-series line profiles and atomic hydrogen excitation rates, *Astrophys. J.*, *452*, 462, 1995.

Meriwether, J. W., Jr., S. K. Atreya, T. M. Donahue, and R. G. Burnside, Measurements of the spectral profile of Balmer alpha emission from the hydrogen geocorona, *Geophys. Res. Lett.*, *7*, 967, 1980.

Mierkiewicz, E. J., F. L. Roesler, J. Bishop, and S. M. Nossal, A systematic program for ground-based Fabry-Perot observations of the neutral hydrogen exosphere, in *Optical Spectroscopic Techniques and Instrumentation for Atmospheric and Space Research III: Proc. Int. Soc. Opt. Eng.*, *3756*, 323, 1999.

Nossal, S., Fabry-Perot observations of geocoronal hydrogen Balmer-α emissions, Ph.D. thesis, Univ. of Wis., Madison, Wis., 1994.

Nossal, S., F. L. Roesler, R. J. Reynolds, and F. Scherb, Solar cycle variations of geocoronal Balmer-α emission, *J. Geophys. Res.*, *98*, 3669, 1993.

Nossal, S., F. L. Roesler, M. M. Coakley, and R. J. Reynolds, Geocoronal hydrogen Balmer-α line profiles obtained using Fabry-Perot annular summing spectroscopy: Effective temperature results, *J. Geophys. Res.*, *102*, 14,541, 1997.

Nossal, S., F. L. Roesler, and M. M. Coakley, Cascade excitation in the geocoronal hydrogen Balmer-α line, *J. Geophys. Res.*, *103*, 381, 1998.

Percival, J. W., Low bandwidth techniques for remote observing (abstract), paper presented at WGAS Session on Remote Observing, 185th Meeting, Am. Astron. Soc., Tucson, Ariz., 1995.

Reynolds, R. J., A measurement of the hydrogen recombination rate in the diffuse interstellar medium, *Astrophys. J.*, *282*, 191, 1984.

Reynolds, R. J., Ionizing the galaxy, *Science*, *277*, 1446, 1997.

Reynolds, R. J., F. L. Roesler, F. Scherb, and J. Harlander, Fabry-Perot/CCD multichannel spectrometer for the study of warm, ionized interstellar gas and extragalactic clouds, in *Instrumentation in Astronomy VII*, *Proc. Int. Soc. Opt. Eng.*, *1235*, 610, 1990.

Reynolds, R. J., S. L. Tufte, L. M. Haffner, K. Jaehnig, and J. Percival, The Wisconsin H-alpha Mapper (WHAM): A brief review of performance characteristics and early scientific results, *Publ. Astron. Soc. Aust.*, *15*, 14, 1998.

Roble, R. G., and R. E. Dickinson, How will changes in carbon dioxide and methane modify the mean structure of the mesosphere and thermosphere?, *Geophys. Res. Lett.*, *16*, 1441, 1989.

Roble, R. G., and E. C. Ridley, A thermosphere ionosphere mesosphere electrodynamics general circulation model (TIME-GCM): Equinox solar minimum circulation (30–500 km), *Geophys. Res. Lett.*, *21*, 417, 1994.

Roesler, F. L., Fabry-Perot instruments for astronomy, in *Methods of*

Experimental Physics, vol. 12, *Part A: Optical and Infrared*, edited by L. Martin and N. Carlton, p. 531, Academic, San Diego, Calif., 1974.

Scherb, F., Hydrogen production rates from ground-based Fabry-Perot observations of comet Kohoutek, *Astrophys. J.*, *243*, 644, 1981.

Shih, P., F. L. Roesler, and F. Scherb, Intensity variations of geocoronal Balmer alpha emission, 1, Observational results, *J. Geophys. Res.*, *90*, 477, 1985.

Tousey, R., Extreme ultraviolet spectrum of the sun, *Space Sci. Rev.*, *2*, 3, 1963.

Tousey, R., J. D. Purcell, W. E. Austin, D. L. Garrett, and K. G. Widing, New photographic spectra of the Sun in the extreme ultraviolet, *Space Res.*, *4*, 703, 1964.

Tufte, S. L., The WHAM spectrometer: Design performance characteristics and first results, Ph.D. thesis, Univ. of Wis., Madison, Wis., 1997.

Warren, H. P., J. T. Mariska, and K. Wilhelm, High-resolution observations of the solar hydrogen Lyman lines in the quiet Sun with the SUMER instrument on SOHO, *Astrophys. J. Suppl. Ser.*, *119*, 105, 1998.

Woods, T. N., and G. J. Rottman, Solar Lyman alpha irradiance measurements during two solar cycles, *J. Geophys. Res.*, *102*, 8769, 1997.

Yelle, R. V., and F. L. Roesler, Geocoronal Balmer alpha line profiles and implications for the exosphere, *J. Geophys. Res.*, *90*, 7568, 1985.

J. Bishop, E. O. Hulburt Center for Space Research, Naval Research Laboratory, Code 7643, 4555 Overlook Avenue, S.W., Washington D. C. 20375.

M. Haffner, R. J. Reynolds, and S. Tufte, Astronomy Department, University of Wisconsin, 475 N. Charter St., Madison, WI 53706.

E. Mierkiewicz, Department of Atmospheric and Oceanic Sciences, University of Wisconsin, 1225 W. Dayton St., Madison, WI 53706.

S. Nossal and F. L. Roesler, Physics Department, University of Wisconsin, 1150 University Ave., Madison, WI 53706. (nossal@wisp5.physics.wisc.edu)

J. Percival, Space Astronomy Laboratory, University of Wisconsin, 1150 University Ave., Madison, WI 53706.

(Received January 5, 2000; revised October 10, 2000;
accepted November 20, 2000.)